

PPPL-3127

Sensitivity of equilibrium reconstruction to motional-Stark-effect measurements

S. H. Batha and F. M. Levinton

Fusion Physics and Technology, Torrance, CA 90503

S. P. Hirshman

Oak Ridge National Laboratory, Oak Ridge, TN 37831

M. G. Bell and R. M. Wieland

Princeton Plasma Physics Laboratory, P.O. Box 451, Princeton, NJ 08543

(Received

The magnetic-field pitch-angle profile, $\gamma_p(R) \equiv \arctan(B_{\text{pol}}/B_{\text{tor}})$, is measured on the Tokamak Fusion Test Reactor (TFTR) [Plasma Phys. Controlled Nucl. Fusion Res. 1, 51 (1987)] using a motional Stark effect (MSE) polarimeter. Measured pitch-angle profiles, along with kinetic profiles and external magnetic measurements, are used to compute a self-consistent equilibrium using the free-boundary Variational Moments Equilibrium Code VMEC. Uncertainties in the q profile due to uncertainties in the $\gamma_p(R)$, magnetic measurements, and kinetic measurements are quantified. Subsequent uncertainties in the VMEC-calculated current-density and shear profiles are also quantified.

PACS Numbers: 52.70.Ds, 52.30.Bt, 52.65.+z, 52.55.Fa

1. INTRODUCTION

Transport, stability, and equilibrium analysis of tokamak plasmas are extremely sensitive to the safety factor (q) profile and to $q(0)$, the value of q at the magnetic axis. Measurement of the internal magnetic field gives direct access to the q profile since the q profile is the inverse of the rotational transform of the magnetic field lines. This measurement is now routinely made using motional Stark effect (MSE) polarimetry on the PBX-M,[1,2] Tokamak Fusion Test Reactor (TFTR),[3] and DIII-D[4] tokamaks. The shear and current-density profiles are also required for stability analyses and are most easily and accurately obtained through an equilibrium reconstruction due to the spatial sparseness of the MSE measurements. To reconstruct the entire plasma equilibrium with a free-boundary equilibrium solver, additional information such as external magnetics and internal kinetics measurements are required.

Because calculations of transport, stability, and equilibrium properties are extremely sensitive to the q profile, a quantitative assessment of the uncertainties of the q , shear, and current profiles is required to determine the uncertainty of the calculations. Previous studies have examined the sensitivity of the reconstructed equilibrium to external measurements of the poloidal field, flux, diamagnetic flux and diamagnetic inductance.[5] The addition of internal poloidal magnetic field measurements greatly reduces uncertainty in the computed equilibria. Line-integrated Faraday rotation measurements provided the first routine measurement of the poloidal field.[6] Their inclusion in reconstructions was considered by Blum *et al.*[7] Lao *et al.*[8] estimated that the uncertainty in $q(0)$ was reduced by a factor of 2 when two spatially localized, internal field measurements constrained the equilibrium. None of these studies directly addressed the important issue of uncertainty in the *shape* of the q , shear, and current profiles. Equilibrium studies on the FTU tokamak found that the addition of kinetic pressure profiles to the magnetics data, without internal magnetic field measurements, could provide a reasonable estimate of the toroidal current density profile.[9]

This paper quantifies uncertainties in the q , shear, and current profiles derived from measurements taken with the MSE diagnostic system on TFTR[10] during the 1992 run. Uncertainties for the 1993-95 run are expected to be the same or reduced slightly due to improved calibration techniques, better optical throughput, and overall optimization of the entire MSE diagnostic system. The process of measuring internal pitch angles and converting to q profile information is described in section 2. The elements of this process include the motional Stark effect polarimeter[3] itself, the TFTR external magnetics set,[11] kinetic data, and the VMEC free-boundary equilibrium reconstruction code.[12] The uncertainties in the q profile, central safety factor, shear profile, and other computed quantities are presented in section 3.

2. IMPLEMENTATION

2.1. Motional Stark Effect Polarimeter

A multi-channel motional Stark effect polarimeter has been installed on TFTR and has been collecting data for several years.[3,13] Briefly, the diagnostic technique exploits the physical phenomenon that an atom traveling across the magnetic field of a tokamak will experience a “motional Stark effect” electric field ($E_{MSE} = \mathbf{V} \times \mathbf{B}$).[14] The electric field produces Stark splitting and polarization parallel to the local magnetic field of the emitted Balmer-alpha radiation. In practice, the magnetic-field pitch angle,

$$\gamma_p \equiv \arctan(B_{pol} / B_{tor}) , \quad (1)$$

is measured, where B_{pol} is the poloidal field and B_{tor} is the toroidal field.

On TFTR, the pitch angle is measured at twelve locations along the equatorial midplane of the tokamak. The measurement volume is limited to the intersection of the collection optics sightline and the neutral-beam path resulting in a radial resolution of about 3 cm. The sightline-to-sightline spacing is known to an accuracy of better than ± 0.2 cm with an absolute uncertainty in the sightline major radius of ± 1.0 cm. In 1992,

10 sightlines were available. For the 1993-95 series of experiments using deuterium and tritium as fuel, two additional sightlines were added for a total of 12. The sightlines span the major radius interval $R_{mag} - 0.3a < R < R_{mag} + a$ along the equatorial midplane, where R_{mag} and a are the magnetic axis and minor radius of the plasma, respectively.

Typical total uncertainties in the MSE pitch angles are shown in figure 1 for both 1992 and 1993-95 data. Statistical uncertainties are estimated directly from the raw data during analysis of each discharge. The pitch angles are usually averaged over a time bin of 3 to 50 msec although the data are collected at 2000 samples per second. Added, in quadrature, to the statistical uncertainties are estimates of the systematic uncertainties obtained from the plasma motion calibration discussed in reference [13]. The uncertainties are greatest at the most inboard sightlines due to vignetting of the collection optics and beam attenuation.

2.2. TFTR Magnetic Diagnostics

The standard set of TFTR magnetic diagnostics[11] is employed during the equilibrium reconstruction using VMEC. These include diamagnetic flux, toroidal flux, plasma current, saddle-coil, and 25 B_θ/B_ρ magnetic loop measurements. Each of these measurements is made outside of the vacuum vessel. Additionally, the values of the currents circulating through the external (toroidal, poloidal, etc.) magnets are required in order to determine the vacuum magnetic field. A summary of the quantities used and their errors is given in Table I.

2.3. Equilibrium Reconstruction with VMEC

The plasma equilibrium at a single time point is reconstructed from the MSE pitch angle data, the external magnetics measurements, and total thermal pressure, including the numerically computed fast-ion beam pressure[15] using the free-boundary Variational Moments Equilibrium Code VMEC.[12] The VMEC code solves the MHD equilibrium

equation, $\mathbf{J} \times \mathbf{B} = \nabla p$, in inverse coordinates using a steepest descent algorithm to minimize the ideal MHD energy. An inverse coordinate representation determines the mapping of the cylindrical coordinates (R, Z) in terms of the flux coordinates (Φ, θ) . Here, Φ is the toroidal flux and θ is the poloidal angle. The MHD energy minimization is performed for *prescribed* pressure (p) and q profiles. To match these profiles to internal kinetics and magnetics data (including MSE data), a second minimization of the data mismatch χ^2 is performed *simultaneously* with the primary MHD minimization. Thus, the steady-state solution to this iterative procedure yields a result which satisfies the equilibrium equations with $p(\Phi)$ and $q(\Phi)$ profiles to minimize χ^2 . Cubic tension splines are used to represent p and q , with the knot locations for q conveniently chosen to coincide with the MSE data points. These knot values are allowed to vary during the MHD energy minimization to obtain a minimum for χ^2 .

A typical VMEC equilibrium for TFTR matches up to 91 measurements of plasma properties such as the plasma current, diamagnetic flux, six saddle coils, twenty-five B_θ , twenty-five B_ρ loops, twenty-one pressure points, and twelve MSE data values. Not all of these measurements are independent, however. The plasma is nearly symmetric in the vertical direction so that approximately half the saddle coils and magnetic field loops are redundant. The total number of independent measurements, N , is 63. A “good” fit typically has a value of χ^2 less than 50, so that $\chi^2/N < 1$.

Besides the standard magnetics information of currents and diamagnetic flux, the code requires, as a minimum, the MSE pitch-angle profile and the pressure profile. Usually, the pressure profile is provided by the time-dependent interpretive transport code[16] TRANSP where the measured ion and electron thermal pressure are combined with the fast-ion beam pressure. The uncertainty in the pressure profile was estimated by performing a series of 30 TRANSP runs with differing numbers of Monte Carlo particles and with the density, visible bremsstrahlung, and electron temperature experimental measurements varied within their uncertainties. It was found that the computed pressure

varied by about 6% except near the center and edge of the plasma where the variations were up to 12% and 40%, respectively. Variations at the center of the plasma are assumed to be due to the finite number of Monte Carlo particles used to model the slowing down and deposition of the neutral-beam particles.[15] Edge variations are attributed to measurement errors associated with low densities.

The sensitivity of VMEC to different combinations of experimental data and to small displacements in its initial starting point has also been tested. Sensitivity to the initial starting point was tested by reconstructing two typical TFTR discharges using all the available experimental data. Then the reconstructed physical data was used as input data for further reconstructions. In this way, a set of input data for which the equilibrium solution is known was generated. This set was then used as a benchmark to compare against other perturbative numerical experiments which are described below.

Table II presents the results of these experiments by showing the normalized root-mean-squared deviation of the reconstructed data from the benchmark data: $\text{rms } X \equiv [(X_{rec}^2 - X_{ben}^2)/X_{ben}^2]^{1/2}$ where X_{rec} is the reconstructed data and X_{ben} is the benchmark result (Case 1) which uses actual experimental data. Shown are the normalized rms differences for the pressure profile (rms Pressure), the MSE profile (rms MSE), the B_θ/B_ρ loop data set (rms B_θ/B_ρ), and the Saddle Coil data set (rms Saddle). The difference between the benchmark and computed diamagnetic flux is tabulated as $\Delta \phi_{diam} \equiv (\phi_{diam}^{rec} - \phi_{diam}^{ben})$.

Case 1 is the original benchmark reconstruction using actual experimental data. Cases 1a and 1b use the reconstructed data from Case 1 as input data testing the sensitivity of VMEC to different initial guesses for the plasma boundary. In principle, the Case 1a and 1b normalized rms differences should be uniformly zero. The extent to which they are not represents the baseline noise level of the VMEC minimization procedure.

The sensitivity of VMEC to the magnetic data was examined in cases 2 through 4 by using the original experimental data and including or excluding some of the magnetic data sets. Cases 2 and 3 represent the elimination of either the B_θ/B_p loops or the saddle coils, respectively, from the Case 1 data set. In Case 4 both data sets are removed. For both shots, the rms Saddle and rms MSE improve very slightly when the B_θ/B_p loops are removed. Conversely, when the saddle loops are removed, the rms MSE increases. In both cases, $\Delta\phi_{diam}$ either stays the same or degrades. When both magnetic data sets are removed, the rms MSE again improves slightly, but $\Delta\phi_{diam}$ degrades. These observations and the observation that no rms difference value decreases significantly as a result of excluding subsets of the data, rule out the possibility that any subset of the magnetic data is inconsistent within a statistical variation.

A sensitivity study was also conducted where the values of the external coil currents, which determine the vacuum field inside the torus, were perturbed by 1% which is twice the experimental uncertainty. No sensitivity to these perturbations was observed.

3. UNCERTAINTY ANALYSIS

Uncertainty analysis of equilibrium scalar quantities such as $q(0)$ as well as profile quantities such as q , current density, and shear, has been performed using VMEC. For each discharge studied, the original data file was replicated a few hundred times with the experimental data varied by a Gaussian distribution having a standard deviation equal to the uncertainty in the measurement. Equilibria were then reconstructed on each perturbed data file using VMEC and the resulting values of many plasma parameters were tabulated. Results of 1000 reconstructions from a single discharge with $I_p = 1.4$ MA (68257 at 4.20 s) are shown in figures 2 through 11. The results from a series of twelve neutral-beam-heated discharges (200 reconstructions per discharge) are given in Table III. These twelve discharges spanned a wide range of operational regimes on TFTR. For example, the plasma current was between 0.5 and 2.0 MA, the neutral-beam power varied between

10 and 23 MW, the diamagnetic flux was between -1 and 40 mWb, $0.4 < \beta_{pol} < 2$, and the density peaking factor, $n_e(0)/\langle n_e \rangle$, was between 1.5 and 3.0. The uncertainty, defined to be the standard deviation, of each measurement was computed for each discharge. The average standard deviation of the twelve discharges for each measurement is presented in Table III.

An important parameter obtained from the equilibrium reconstruction is $q(0)$. Figure 2 demonstrates that this measurement is very robust, having a standard deviation of 5.2% for this discharge. Table III shows that the average uncertainty of $q(0)$ measured by MSE in this ensemble of discharges is 6%. The impact of statistical, and to some extent systematic, uncertainty in the measurements is reduced because VMEC uses a global fit to all of the poloidal field measurements, effectively averaging over several MSE measurements.

The determination of the diamagnetic flux is not as robust, however. Figure 3 shows that the average difference between the measured and calculated diamagnetic flux is almost -1.0 mWb, at the accuracy of the magnetic measurement (see Table I). The standard deviation is 1.74 mWb, nearly twice the accuracy of the measurement. This difficulty in matching the magnetics measurement is typical of the data examined in this study, see Table III. The positions of the geometric and magnetic axis are resolved to an uncertainty of ± 2.1 cm and ± 1.6 cm, respectively, as demonstrated in figure 4.

To determine the dominant sources of uncertainty, the sensitivity of the reconstruction to the uncertainty of subsets of the experimental data was examined. An important parameter is the diamagnetic flux, ϕ_{diam} , which has been used in some cases to improve the stability of the solution in circular geometry[17] and to compute separately the values of β_{pol} and the internal inductance (l_1) from Shafranov surface integrals.[18] It was found for the TFTR plasmas considered here that the input value of the diamagnetic flux was an unimportant measurement for determining global plasma parameters. Changes in any of the computed quantities were less than 2% when the input value

of ϕ_{diam} was varied by ± 4 mWb, where typical values of ϕ_{diam} are between -1 and 40 mWb.

The edge toroidal flux, ϕ_{tor} , has a stronger effect, but only on the plasma volume and related quantities, such as the geometric axis, surface area, and stored energy. In figure 5, the results of a study where the input value of the edge flux was varied by ± 4 Wb are shown. It is readily apparent that $q(0)$ and R_{mag} are unaffected but that the position of the geometric axis varies by ± 6 cm from the nominal value of 2.61 m over this range of flux. The VMEC equilibria reported in this paper used the value of ϕ_{tor} calculated by a current-filament model[19] and no constraints were put on the size of the plasma by the position of the limiters. It is worth noting that each of the computed equilibria in figure 5 are equally good. That is, the value of χ^2/N is approximately the same and is less than 1 for each value of the edge toroidal flux, no matter how far from the value determined by the current-filament analysis.

A further set of studies was performed where subsets of the experimental data were varied according to their uncertainty, as above, but the rest of the experimental data were held fixed at their measured values. Three data subsets were varied: the pressure data, the magnetics data including all coil currents and flux measurements, and the MSE data. Figure 6(a) shows that the dominant contributors to the uncertainty in $q(0)$ are the MSE measurements. The pressure and magnetics data alone would lead to a different value of $q(0)$, but have little effect on the uncertainty of $q(0)$ when MSE data of sufficient spatial resolution is also present. The increase in $q(0)$ when only the MSE data was varied is due to the different relative uncertainty of the MSE data points on each side of the magnetic axis which are dominant the determination of $q(0)$. These results are consistent with previous studies done with simulated data.[7,8]

The positions of the magnetic and geometric axes are sensitive to all three subsets of the data, figure 6(b). The magnetic axis is relatively insensitive to the magnetics data, but responds to the uncertainty in the pressure and MSE data. The MSE data can

independently determine the location of the magnetic axis since the axis is located at the position where the pitch angle is zero. Similarly, the peak of the pressure profile can determine the location of the axis, assuming that the plasma rotation is small. The geometric axis does not respond to the MSE data, but does respond to the uncertainty in the pressure and magnetics data. The dependence on the magnetics data was also seen in figure 5. The pressure data affect the geometric axis position because the pressure profile includes an implicit measurement of the plasma minor radius given by the peak and edge pressure locations.

Important information for stability and transport analyses are the profiles of q , the current density (j), and shear. The profiles are calculated along the midplane of the plasma which is assumed to be the plane of vertical (up-down) symmetry. Figure 7 displays the baseline q profile for discharge 68257. The error bars represent the standard deviation of the computed q values at the radial locations of the MSE measurements. The standard deviations can be as little as 5% of the q value near the center of the plasma increasing to $\approx 10\%$ near the edge of the plasma.

Similar displays of the current-density and shear profiles are shown in figures 8 and 9, respectively. The shear is defined as [20]

$$Shear = \frac{2V}{q} \frac{\partial q}{\partial \psi} \frac{\partial \psi}{\partial V}, \quad (2)$$

where V is the plasma volume and ψ is the poloidal flux. This definition of shear reduces to the more common $(r/q)\partial q/\partial r$ for a circular plasma in the limit of large aspect ratio. The uncertainty in the j profile is small, of the order of 10% but increasing slightly at the edge where the current is small. The uncertainty in the shear profile is also small, being less than ± 0.15 for $r < 0.8a$. These uncertainties are the same, whether the analysis is performed at constant major radius, as shown in figures 7 - 9, or at constant toroidal flux.

The sensitivity of the q and shear profiles at $r \approx a/4$ to the uncertainty in subsets of the data is displayed in figure 10. In figure 10(a), the value of q at $R = 3.00$ m is more

sensitive to the uncertainties in the pressure and magnetics data than is $q(0)$, given in figure 6(a). The uncertainty in the MSE data is the dominant source of uncertainty for $q(R)$. Inclusion of the MSE data is essential: Without this information, the code would consistently determine a value of $q(R=3.00 \text{ m})$ that is too small. The pressure profile is an important source of uncertainty for the shear at $R = 3.00 \text{ m}$, figure 10(b), contributing about half as much uncertainty as the MSE measurements.

The uncertainty in the MSE data affects the shapes of the calculated profiles as well as the scalar quantities shown in figure 10. The relationship between $q(0)$ and the values of q and shear at $R = 3.00 \text{ m}$ is shown in figure 11. Recall that all three of these quantities are results of the equilibrium reconstruction, not prescribed parameters. The pressure and magnetics data subsets cause the magnitude of q and shear to vary over about 1/4 the range shown in the figures. As shown in figure 6, the value of $q(0)$ does not vary. The MSE data, however, cause almost all of the variation in q , shear, and $q(0)$. The relationship among these three quantities is apparent. The value of the shear decreases because the edge value of q is fixed while $q(0)$ is increasing, leading to a “flatter” profile (lower shear) in the center of the plasma.

4. DISCUSSION AND CONCLUSION

This analysis has concentrated on several TFTR discharges with $0.75 < q(0) < 2.3$. A more demanding test of the diagnostic system is to examine discharges that deviate significantly from the standard operational space of TFTR. Such discharges include high β_{pol} regimes achieved through current ramping[21] as well as rotating plasmas.[13] Great difficulty in matching the external magnetic loops and saddle coils has been encountered for high- β_{pol} discharges where the plasma developed a separatrix as opposed to being a limited plasma.[21] This is speculated to be due to currents outside the separatrix. The main difficulty is in matching the external magnetic loops and saddle

coils. This remains an active area of research. In addition, the effects of plasma rotation and the distinction between parallel and perpendicular pressure may help to mitigate the difference between the computed and observed measurements. Neither of these physical affects are included in the present, data-matching version of VMEC.

A great deal of effort has been expended to provide an accurate calibration of the MSE pitch angle measurement and to reduce the uncertainty in the measurement from 0.5° to 0.2° . [13] Figure 12 shows that the uncertainty in the value of $q(0)$ is dependent on the uncertainty assigned to the MSE pitch angle data. For each data point in figure 12, the uncertainty of each pitch angle datum was assigned to the value shown on the abscissa, then an ensemble of 200 equilibria were reconstructed by VMEC with each experimental datum perturbed within its uncertainty. Two discharges were considered. The first, 68257 (\bullet), is a typical TFTR supershot and has been analyzed in figures 2 - 11. The uncertainty in $q(0)$ increases from 5.2% with the actual uncertainties to more than 30% for an uncertainty in the pitch angle measurement of 1.25° . The second discharge, 69217 (\blacktriangle), is a low current, $I_p = 500$ kA, high $\beta_{pol} \approx 2$ discharge. The uncertainty in $q(0)$ with the actual pitch angle uncertainties is acceptable, 7.1%, but rapidly increases to greater than 40% for a pitch angle uncertainty of 0.75° . Not only does the accuracy decrease as the uncertainty rises, but the ability of the equilibrium code to converge also decreases for the high- β_{pol} discharges. With actual uncertainties, all of the equilibria converged. Only 70% of the code runs converged when the uncertainty was 0.75° .

In conclusion, a motional Stark effect polarimeter to measure the internal magnetic field direction at the plasma midplane has been installed on TFTR. When combined with the standard magnetics diagnostics and the equilibrium code VMEC, a powerful tool is available to analyze q , current density, and magnetic shear profiles. This paper has focused on the uncertainty in the profile quantities based on experimental measurements. It is found that the computed value of $q(0)$ is very robust with an uncertainty of 6% at the one standard deviation level. Likewise, the uncertainties in the $q(R)$, current density, and

shear profiles, which are important for transport and stability analyses, are also small. The primary source of uncertainty in the profiles determined by the equilibrium solver is the uncertainty of the magnetic field pitch angle measurement. However, without these measurements, a different, incorrect equilibrium would be computed. The small uncertainties actually achieved are due to the precision of the pitch angle and other measurements.

ACKNOWLEDGMENTS

The authors would like to acknowledge many useful conversations with M. Mael, R. V. Budny, the software support of J. Felt, and the support of D. W. Johnson, K. M. Young, K. M. McGuire, and M. C. Zarnstorff. This work was supported by the U. S. Department of Energy Contract No. DE-AC02-76-CHO-3073.

REFERENCES

1. F. M. Levinton *et al.*, *Rev. Sci. Instrum.* **61**, 2914 (1990).
2. F. M. Levinton *et al.*, *Phys. Rev. Lett.* **63**, 2060 (1989).
3. F. M. Levinton, *Rev. Sci. Instrum.* **63**, 5157 (1992).
4. D. Wroblewski and L. L. Lao, *Rev. Sci. Instrum.* **63**, 5140 (1992).
5. E. Lazzaro and P. Mantica, *Plasma Physics and Controlled Fusion* **30**, 1735 (1988).
6. H. Soltwisch, *Plasma Physics and Controlled Fusion* **34**, 1669 (1992).
7. J. Blum *et al.*, *Nucl. Fusion* **30**, 1475 (1990).
8. L. L. Lao *et al.*, *Nucl. Fusion* **30**, 1035 (1990).
9. F. Alladio and P. Micozzi, *Nucl. Fusion* **35**, 305 (1995).
10. R. J. Hawryluk *et al.*, in *Plasma Physics and Controlled Nuclear Fusion Research 1986* (Proc. 11th Int. Conf. Kyoto, 1986) Vol. 1, IAEA, Vienna (1987) 51.
11. J. Coonrod *et al.*, *Rev. Sci. Instrum.* **56**, 941 (1985).
12. S. P. Hirshman *et al.*, *Phys. Plasmas* **1**, 2277 (1994).
13. F. M. Levinton *et al.*, *Phys. Fluids B* **5**, 2554 (1993).
14. E. U. Condon and G. H. Shortly, *The Theory of Atomic Spectra* (Cambridge University Press, Cambridge, 1963).
15. R. J. Goldston *et al.*, *J. Comp. Phys.* **43**, 61 (1981).
16. R. J. Hawryluk, presented at the Proc. of the Course on Physics of Plasma Close to Thermonuclear Conditions, Brussels (CEC, 1980), p. 19.
17. Y. K. Kuznetsov *et al.*, *Nucl. Fusion* **26**, 369 (1986).
18. L. Lao *et al.*, *Nucl. Fusion* **25**, 1421 (1985).
19. D. W. Swain and G. H. Neilson, *Nucl. Fusion* **22**, 1015 (1982).
20. H. Takahashi *et al.*, *Nucl. Fusion* **32**, 815 (1992).
21. S. A. Sabbagh, *Bull. Am. Phys. Soc.* **38**, 1984 (1993).

Table I. Estimates of uncertainties for external magnetics measurements.

Quantity	Symbol	Uncertainty	Units
Diamagnetic flux	ϕ_{diam}	± 1 mWb	Wb
Plasma current	I_p	$\pm 0.7\%$	MA
External coil currents		$\pm 0.5\%$	kA
Saddle Coils		± 30 mWb	Wb
B_θ/B_ρ loops		5% typical	T

Table II. Normalized rms deviation between the equilibrium-calculated values and either the measured or the benchmark Case 1, show the sensitivity of VMEC reconstructions using various combinations of perturbed input data: Case (1) experimental data, (1a) and (1b) different plasma boundary guesses and reconstructed data, (2) no B_θ/B_ρ loops used in Case 1 reconstruction, (3) no saddle coils used in Case 1 reconstruction, and (4) neither B_θ/B_ρ loops nor saddle coils used in Case 1 reconstruction. NF = not fit in this case.

Shot	Case	Type	rms Pressure	rms MSE	rms B_θ/B_ρ	rms Saddle	$\Delta\phi_{diam}$ (mWb)
65610	1	benchmark	0.017	0.025	0.035	0.033	0.823
	1a	vary initial conditions	0.010	0.004	0.007	0.013	0.166
	1b	vary initial conditions	0.011	0.005	0.005	0.004	0.187
	2	benchmark, no B_θ/B_ρ	0.017	0.023	NF	0.028	0.800
	3	benchmark, no Saddle	0.017	0.028	0.035	NF	0.879
	4	benchmark, no B_θ/B_ρ or Saddle	0.017	0.021	NF	NF	0.940
68257	1	benchmark	0.019	0.044	0.037	0.042	1.695
	1a	vary initial conditions	0.008	0.011	0.006	0.002	-0.127
	1b	vary initial conditions	0.009	0.012	0.006	0.004	-0.072
	2	benchmark, no B_θ/B_ρ	0.020	0.041	NF	0.035	1.794
	3	benchmark, no Saddle	0.020	0.043	0.038	NF	1.768
	4	benchmark, no B_θ/B_ρ or Saddle	0.020	0.041	NF	NF	1.910

Table III. Uncertainties of various calculated quantities (averaged over 12 discharges).

Quantity	Symbol	Standard Deviation	Units
Magnetic Axis	R_{mag}	1.6	cm
Geometric Axis	R_{geo}	2.1	cm
Stored Energy	W	9%	MJ
Difference in Diamagnetic Flux (Measured-Calculated)	$\Delta\phi_{diam}$	1.7	mWb
Internal Inductance	l_i	11%	
Diamagnetic Energy	μ_i	0.08	
Safety Factor	q(0)	6%	
Edge q	q(a)	11%	
Volume	V	6%	m ³

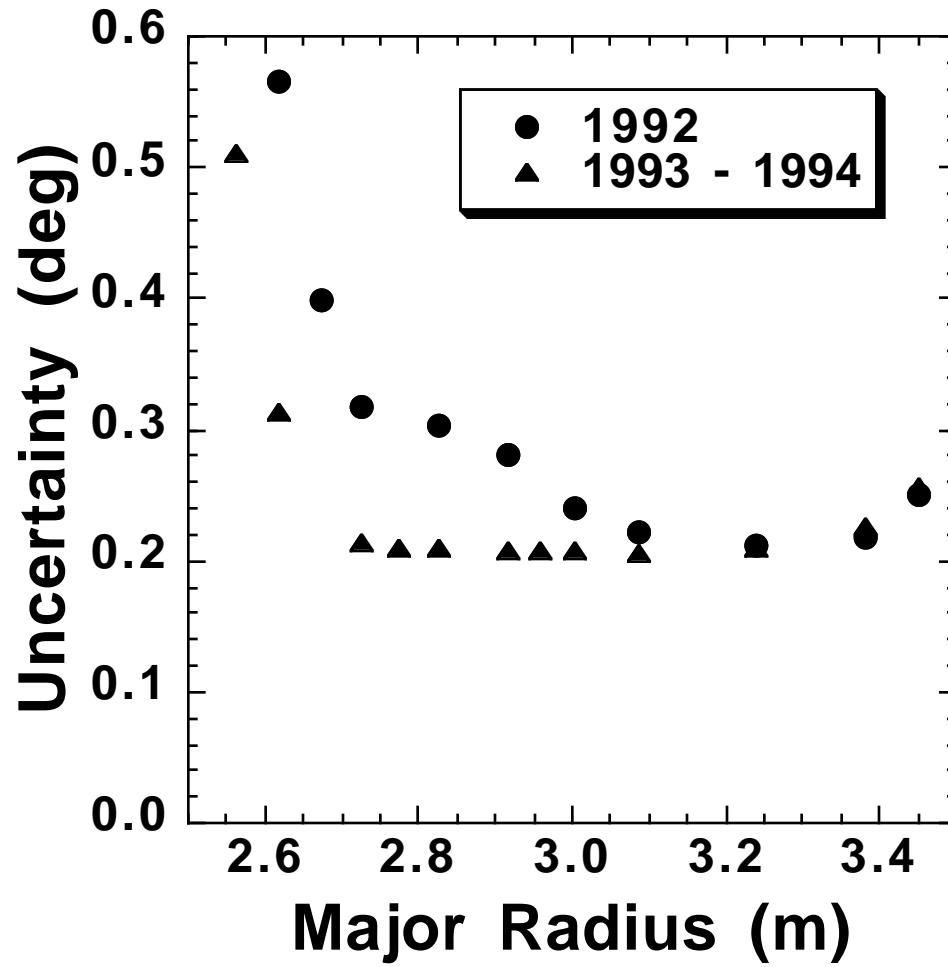


Figure 1. The total (systematic and statistical) uncertainty of the MSE-measured pitch angle data for 1992 (•) and 1993-94 (▲).

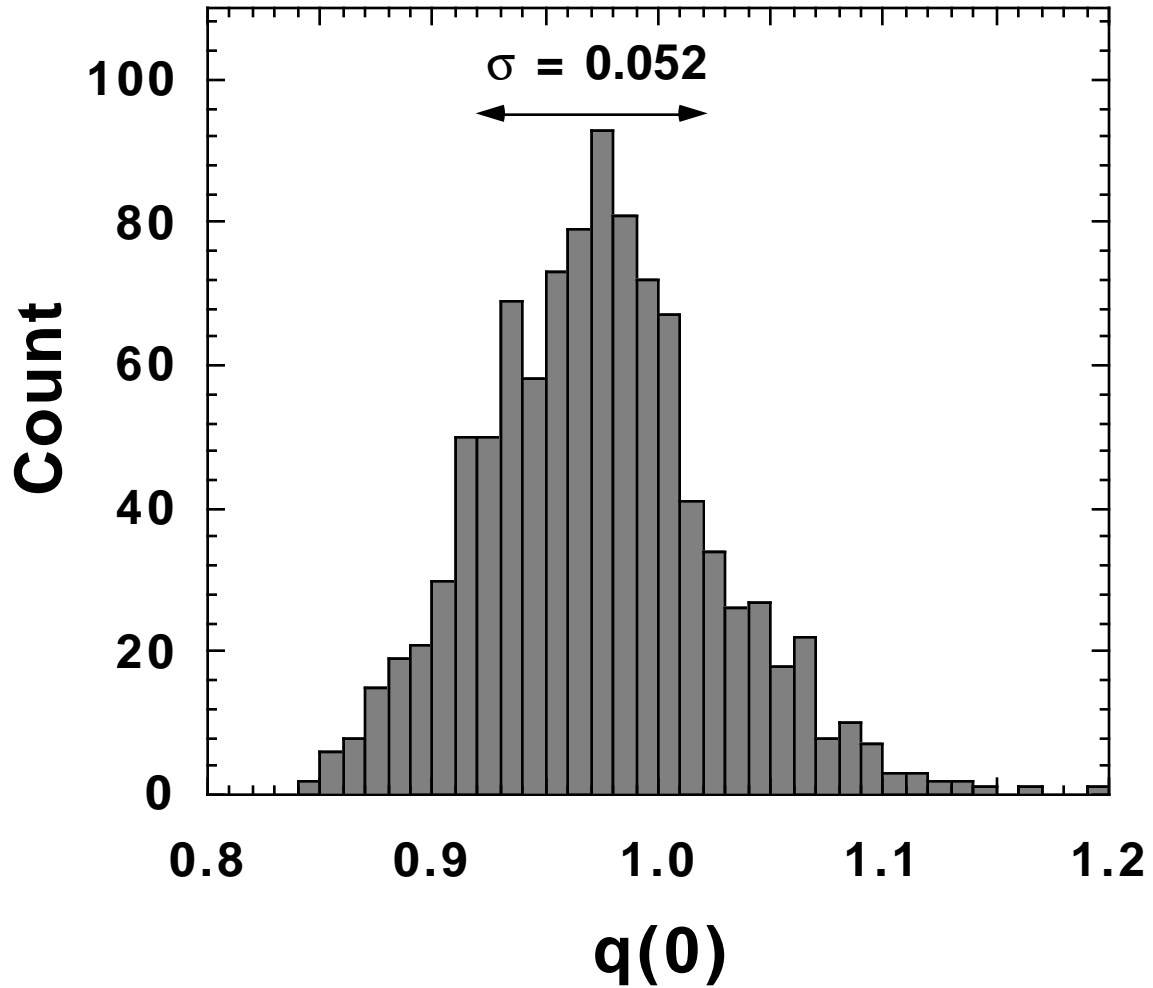


Figure 2. Distribution of the calculated $q(0)$ for discharge 68257. The value of $q(0)$ determined from the experimental data was 0.966. An ensemble of 1000 equilibria reconstructed by VMEC, where each experimental datum was perturbed by its uncertainty, calculated the average value of $q(0)$ to be 0.973 with a standard deviation of 5.2%.

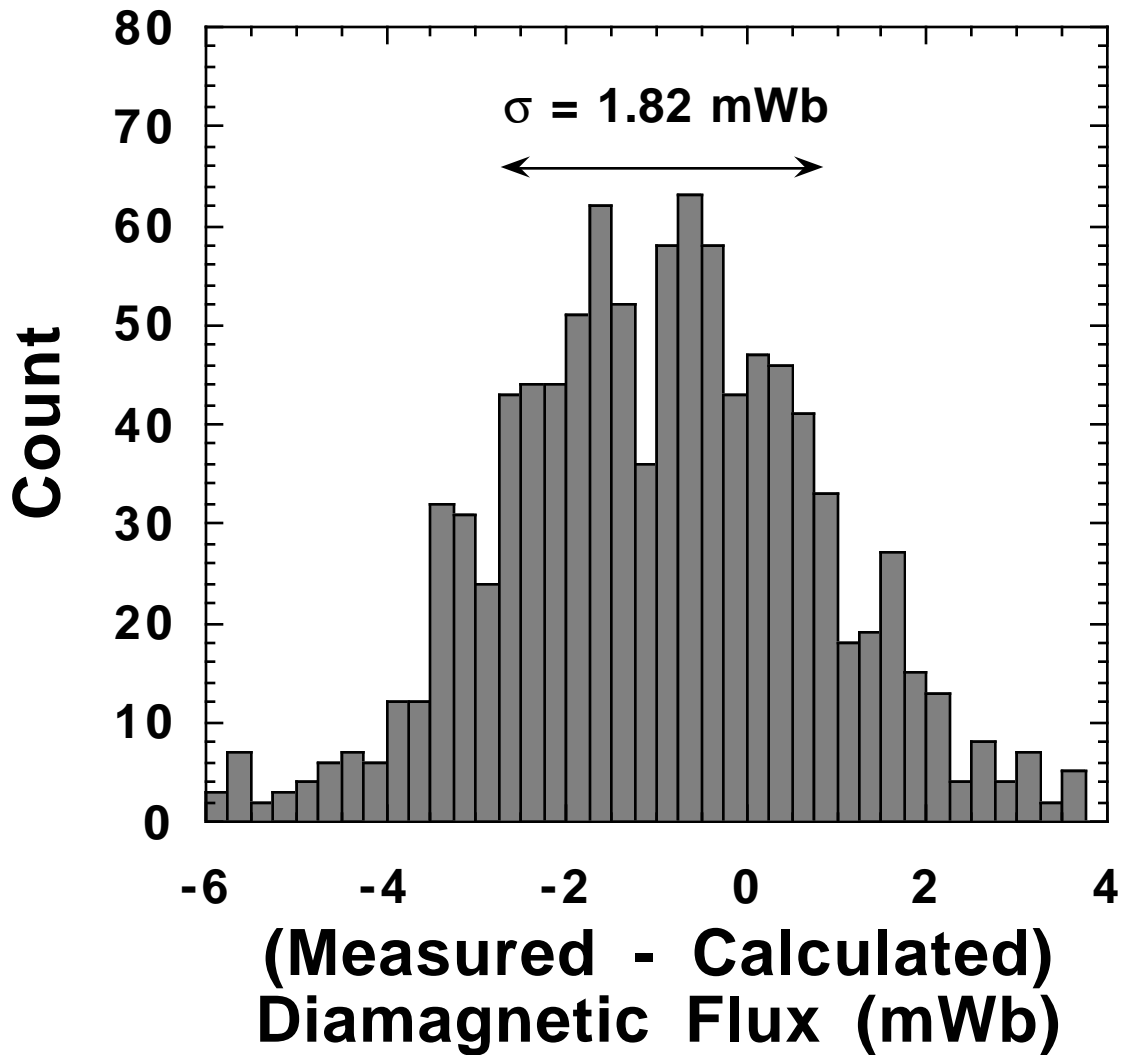


Figure 3. Distribution of the difference between the measured and calculated diamagnetic flux, $\Delta\phi_{diam}$, for discharge 68257. An ensemble of 1000 equilibria reconstructed by VMEC, where each experimental datum was perturbed by its uncertainty, calculated the average value of $\Delta\phi_{diam}$ to be -1.00 mWb with a standard deviation of 1.82 mWb.

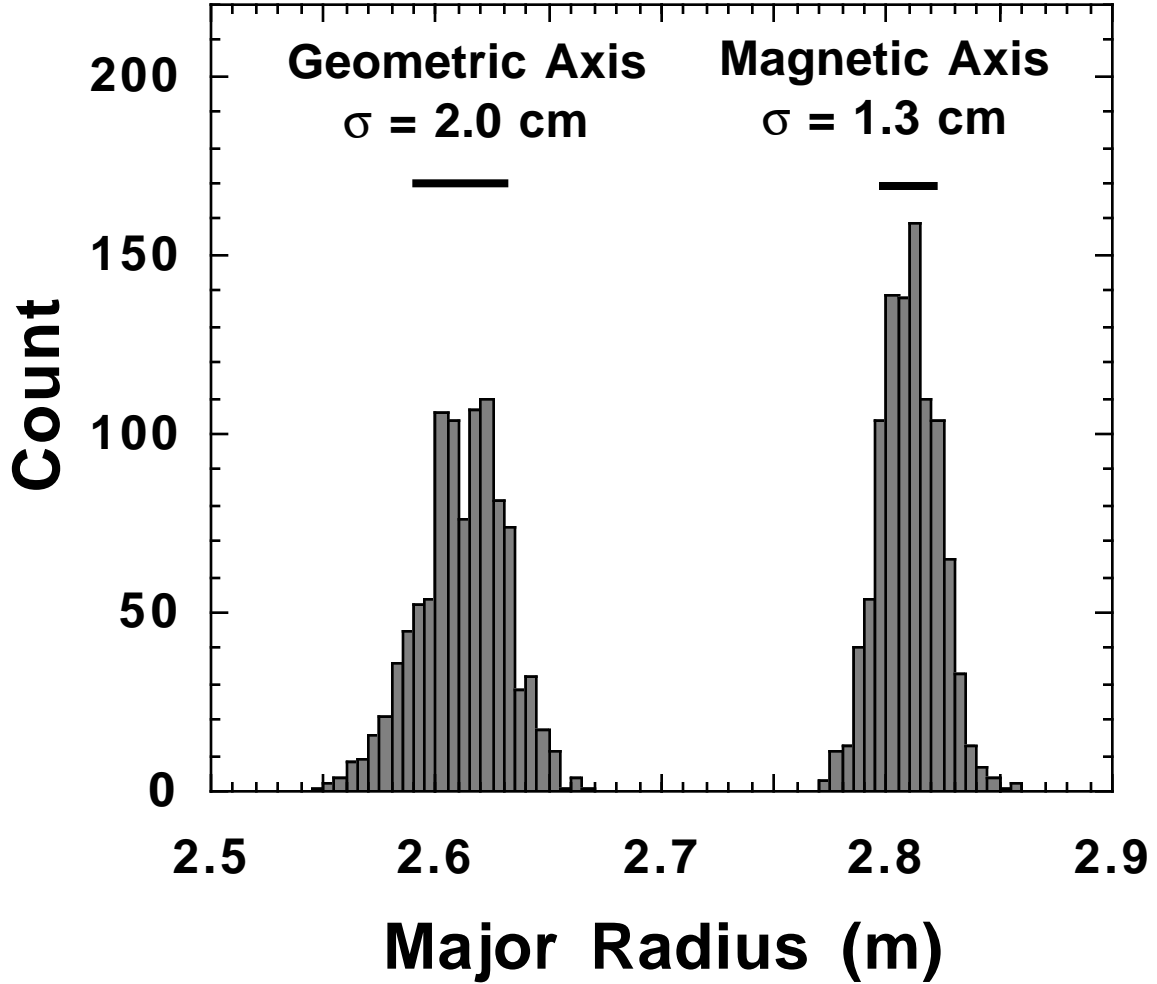


Figure 4. Distribution of the calculated values of the geometric (R_{geo}) and magnetic (R_{mag}) axes for discharge 68257 at 4.2 s. The baseline value of R_{geo} was 261.1 cm while an ensemble of 1000 equilibria reconstructed by VMEC, with each experimental datum perturbed by its uncertainty, calculated the average R_{geo} to be 261.2 cm with a standard deviation of 2.0 cm. The baseline value of R_{mag} was 281.4 cm while the average R_{mag} was 281.0 cm with a standard deviation of 1.3 cm. The thick lines show twice the standard deviation.

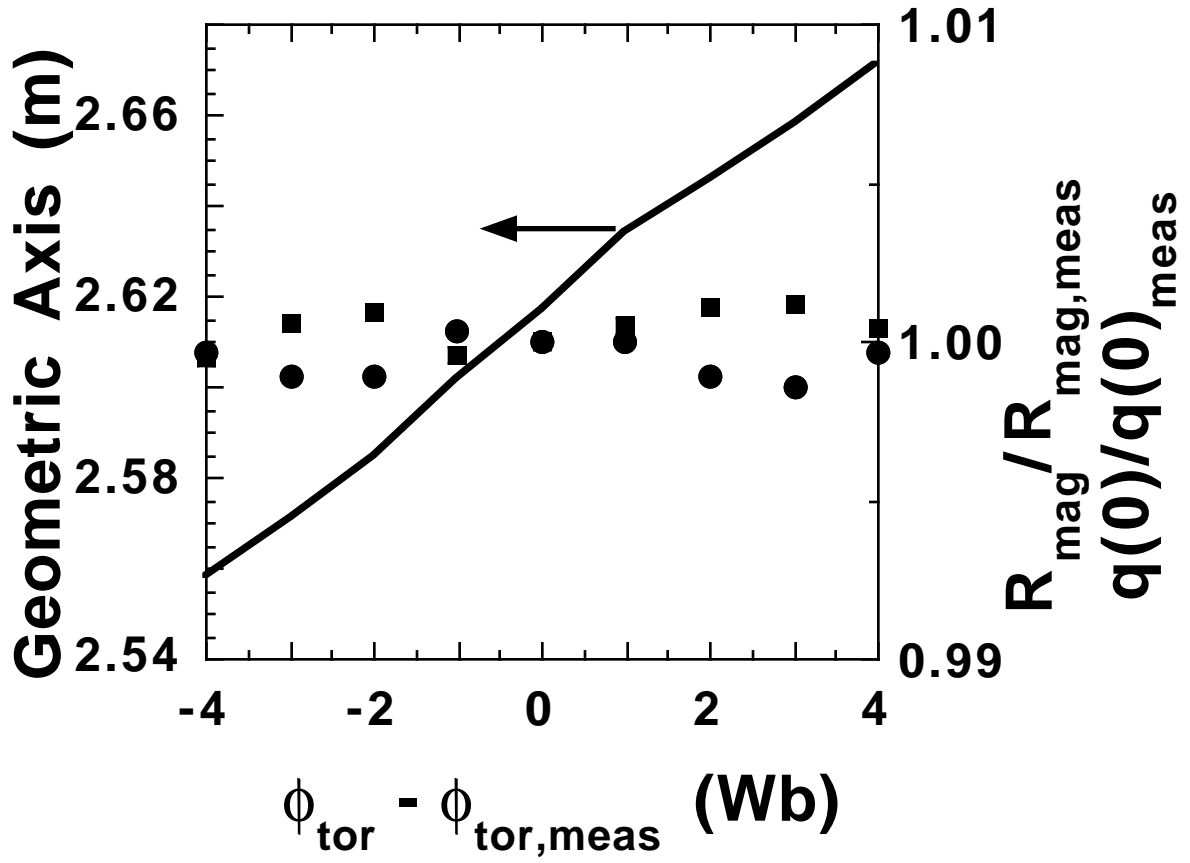


Figure 5. The equilibrium for discharge 68257 at 4.2 s was computed several times with different values of the edge toroidal flux. The major difference is the position of the geometric axis of the plasma and related quantities such as plasma volume, stored energy, and internal inductance. The position of the magnetic axis and the value of $q(0)$, shown normalized to their values at the measured value of the flux, are not sensitive to variations in the flux.

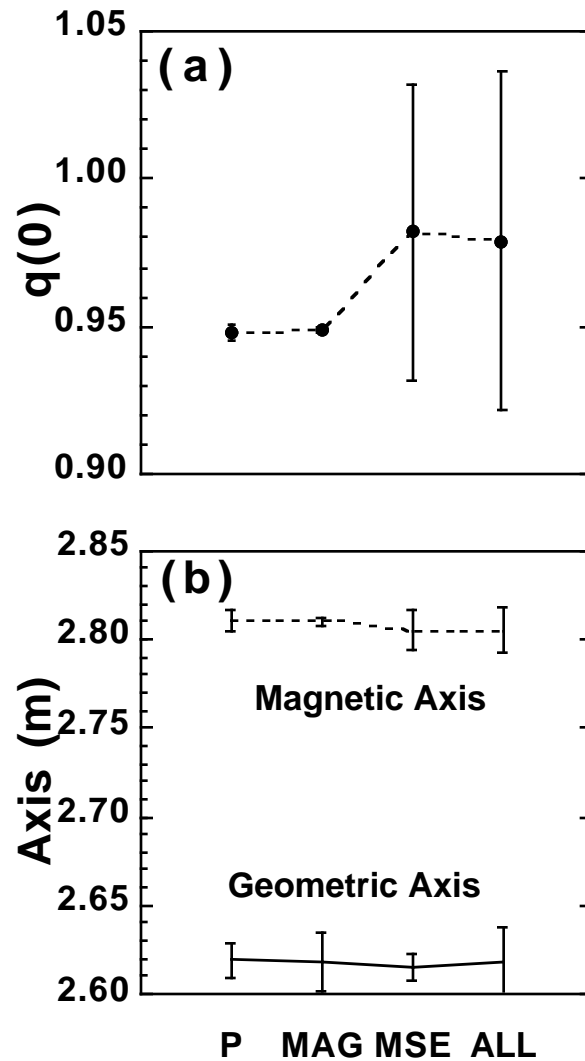


Figure 6. The average value and uncertainty of (a) $q(0)$ and (b) the magnetic and geometric axis locations when subsets of the experimental data from a single discharge were varied while all other measurements were held at their measured values. Varied were the pressure data (P), all of the magnetics data including coil currents and flux measurements (MAG), and the MSE measurements including systematic uncertainties of pitch angle and radial location (MSE). Also included is the result when all of the measured quantities were varied within their uncertainties (ALL).

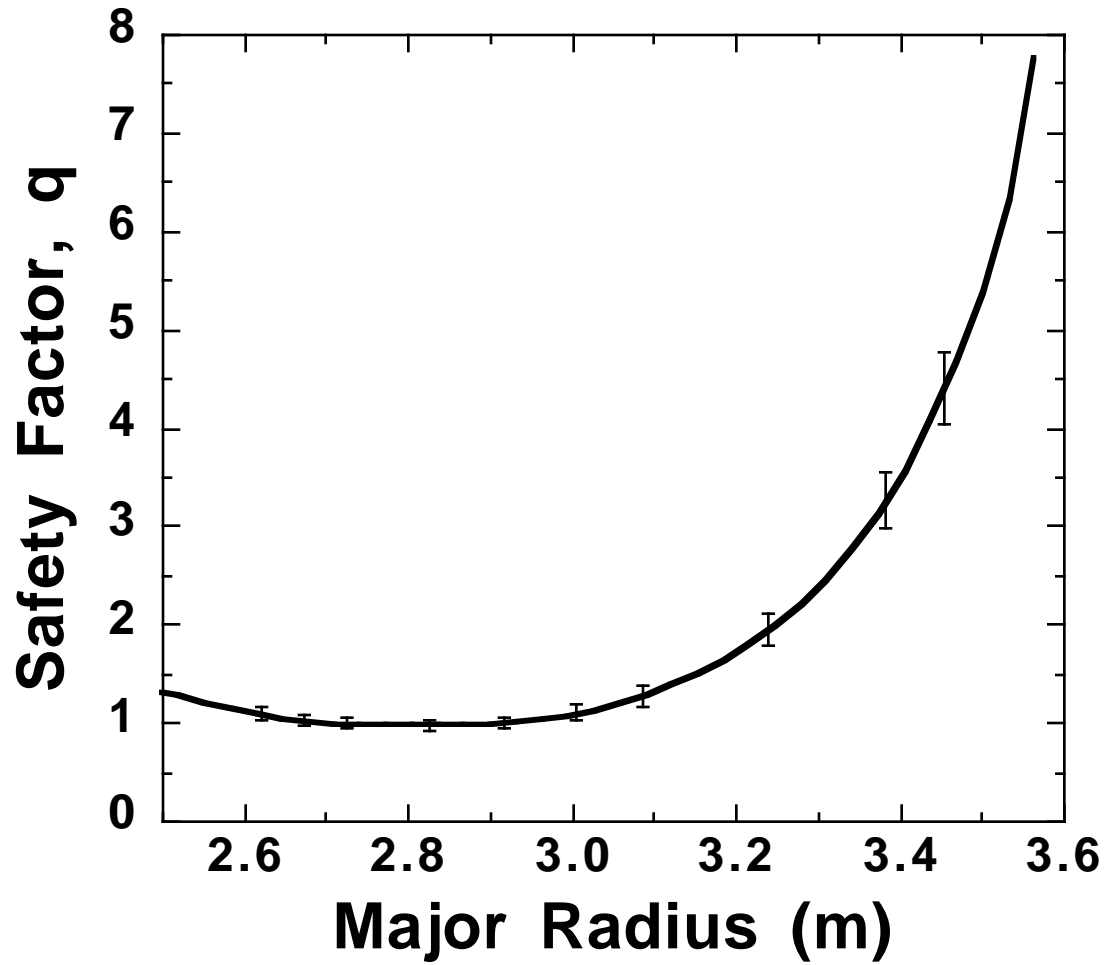


Figure 7. The computed baseline $q(R)$ profile for discharge 68257. The error bars represent the standard deviation calculated from an ensemble of 1000 equilibria reconstructed by vmec, where each experimental datum was perturbed within its uncertainty.

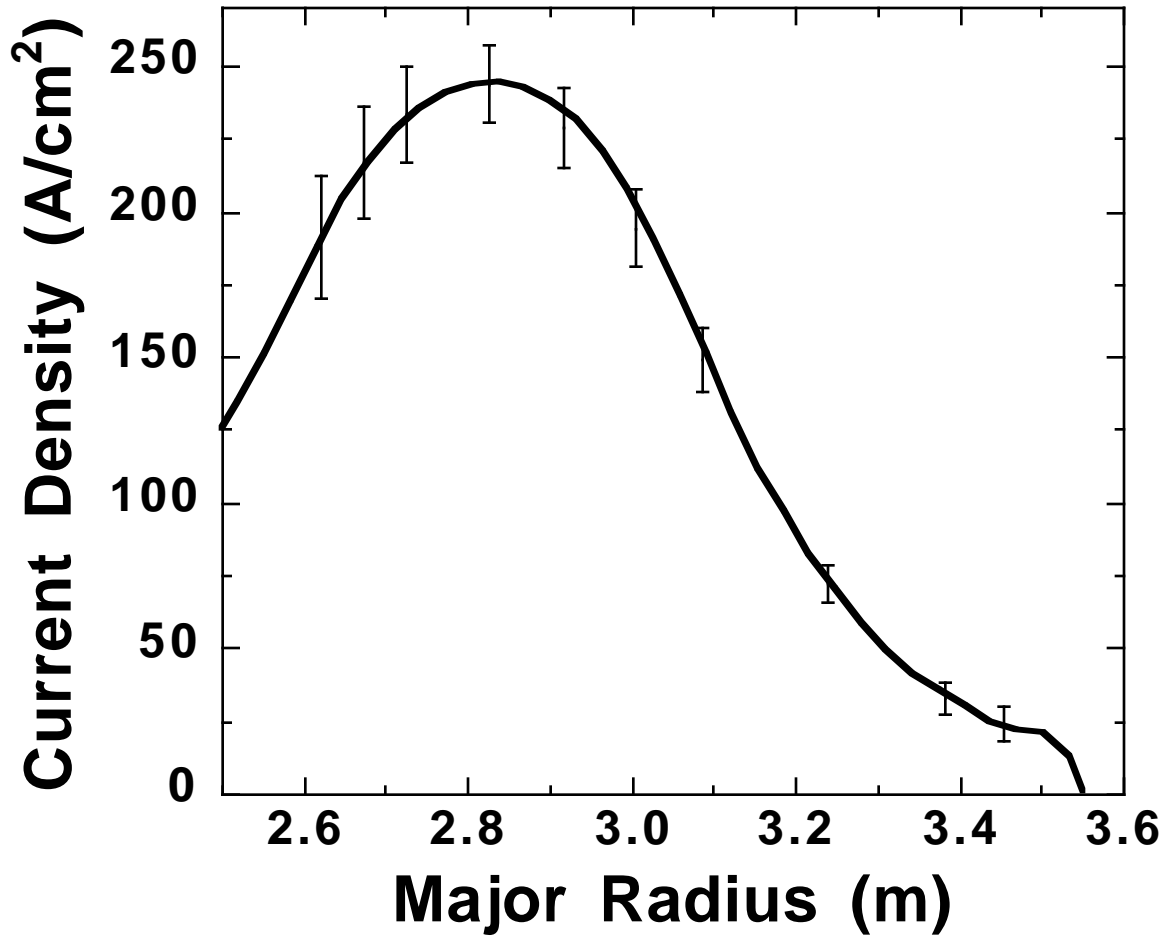


Figure 8. The computed baseline current-density profile, $j(R)$, for discharge 68257. The error bars represent the standard deviation calculated from an ensemble of 1000 equilibria reconstructed by VMEC, where each experimental datum was perturbed within its uncertainty.

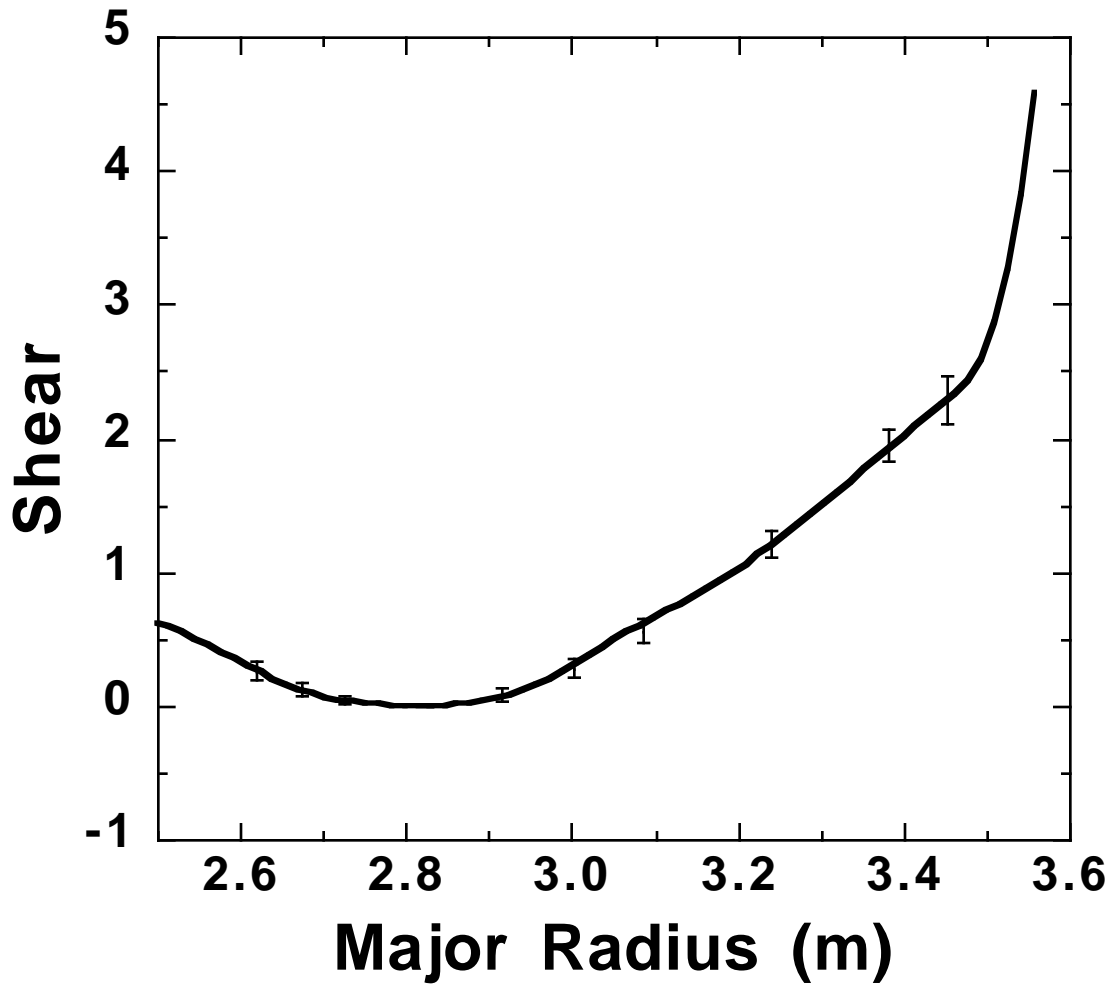


Figure 9. The computed baseline shear profile for discharge 68257. The error bars represent the standard deviation calculated from an ensemble of 1000 equilibria reconstructed by VMEC, where each experimental datum was perturbed within its uncertainty.

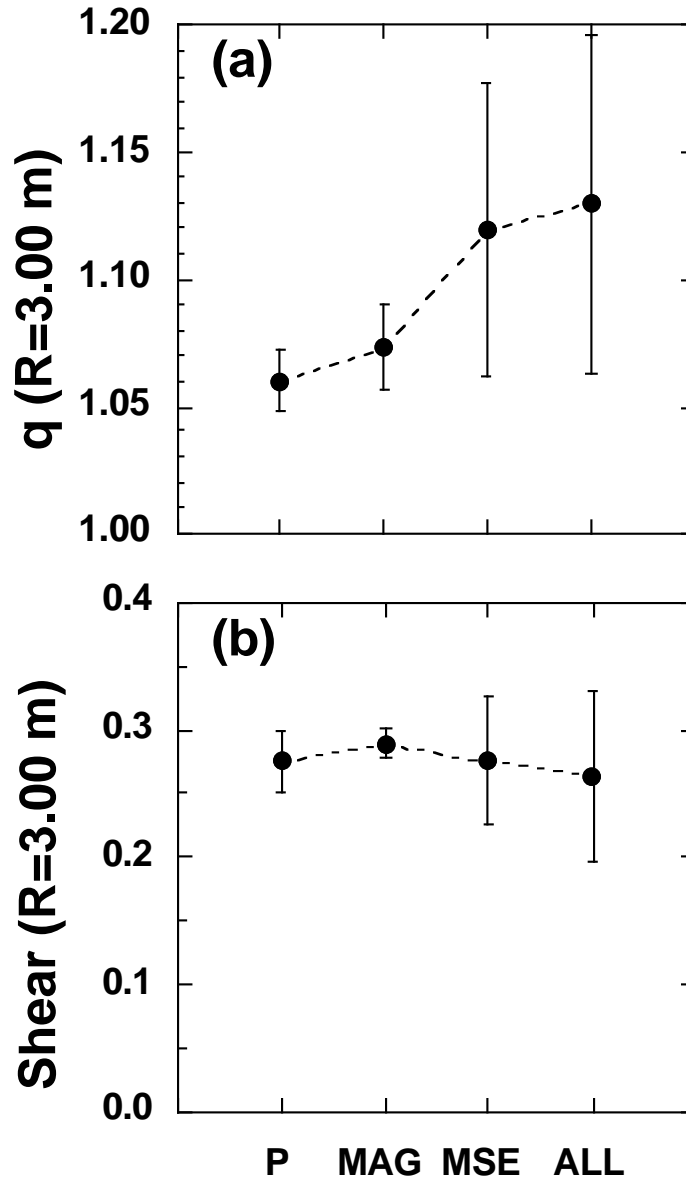


Figure 10. The value and uncertainty of (a) q and (b) shear at a major radius of 3.00 m when subsets of the experimental data were varied while all other measurements were held at their measured values. Varied were the pressure data (P), all of the magnetics data including coil currents and flux measurements (MAG), and the MSE measurements including systematic uncertainties of pitch angle and radial location (MSE). Also included is the result when all of the measured quantities were varied within their uncertainties (ALL).

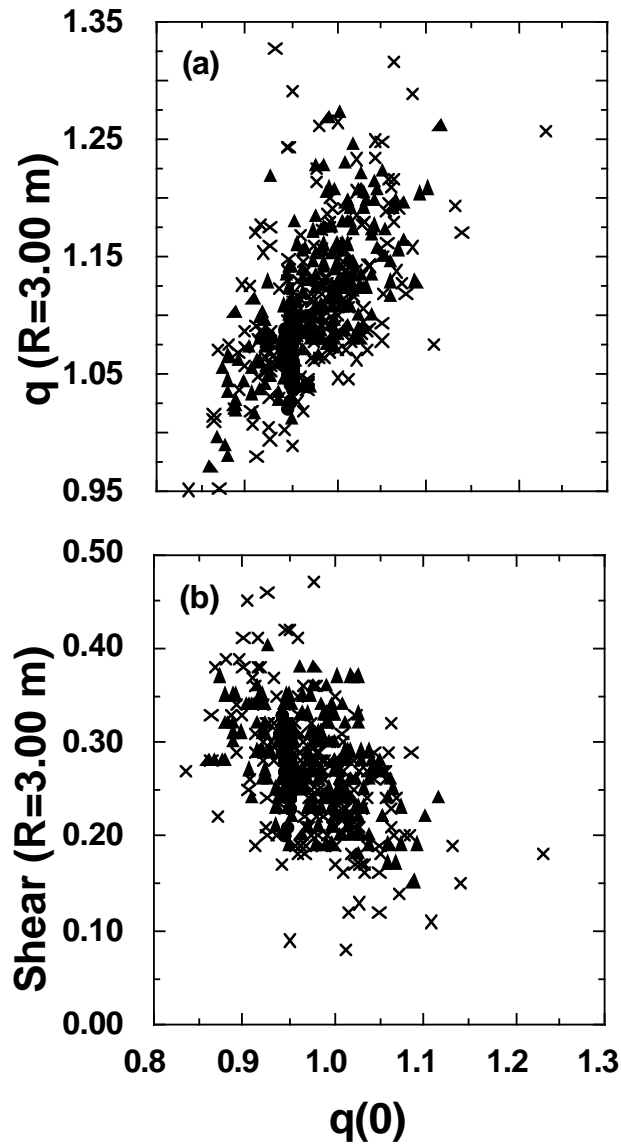


Figure 11. The relationship between $q(0)$ and (a) q and (b) shear at a major radius of 3.00 m when subsets of the experimental data were varied. The pressure data (\bullet) and all of the magnetics data including coil currents and flux measurements ($+$) were varied. These data points are all within the dense collection of points at $q(0) \approx 0.95$. Also included are the result of varying the MSE measurements including systematic uncertainties of pitch angle and radial location (\blacktriangle) and the result when all of the measured quantities were varied within their uncertainties (\times). These data were summarized in figure 10.

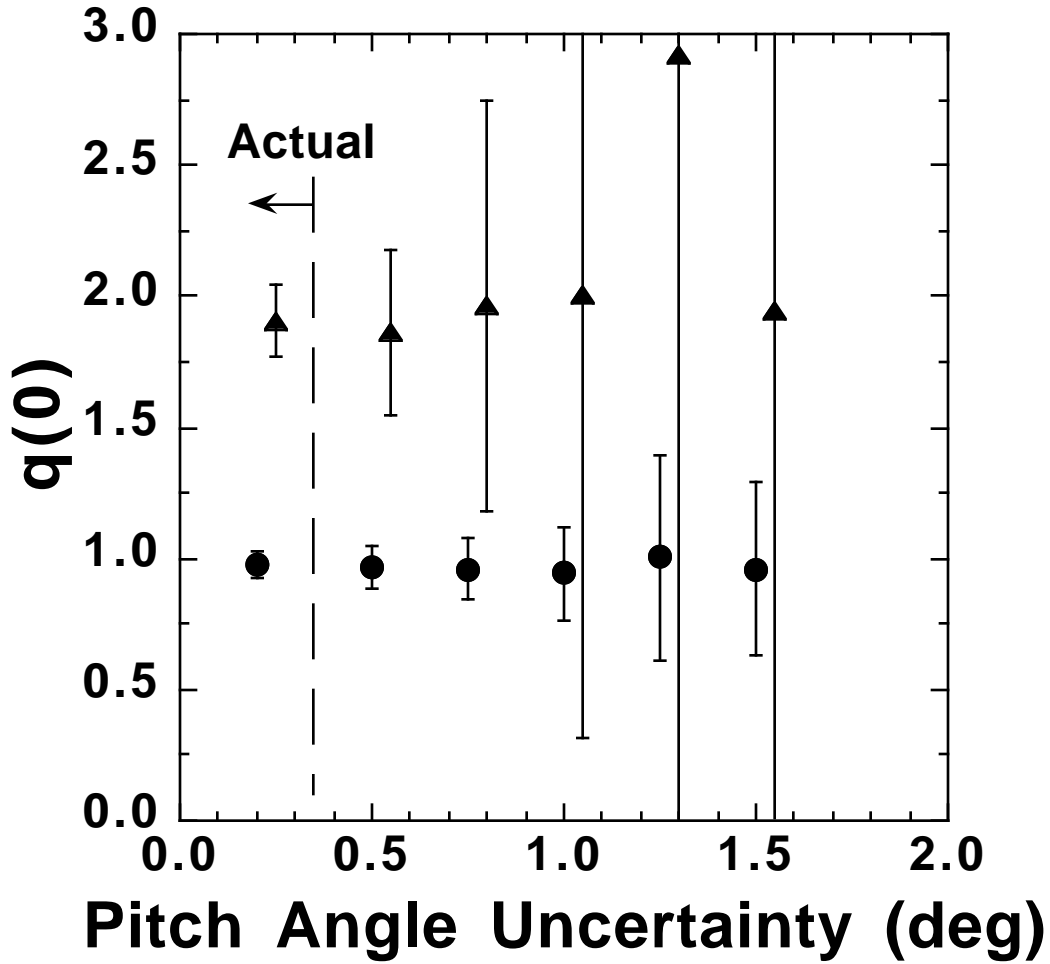


Figure 12. The value of $q(0)$ varies and the uncertainty of $q(0)$ increases dramatically as the uncertainty in the measurement of the magnetic field pitch angles increases. Shown are the effects for a typical supershot discharge, 68257 (\bullet), and a discharge with high β_{pol} , 69217 (\blacktriangle). The data for 69217 have been shifted in uncertainty by $+0.05^\circ$ to avoid overlapping the other data. The points labeled “actual” used the uncertainties shown in figure 1. The error bars represent the standard deviation calculated from an ensemble of 200 equilibria reconstructed by VMEC, where each experimental datum was perturbed within its uncertainty.